Optics & Laser Technology 88 (2017) 275–279

Contents lists available at ScienceDirect

Optics & Laser Technology

journal homepage: www.elsevier.com/locate/optlastec

Full length article

Passive Q-switching of $Pr:LiYF_4$ orange laser at 604 nm using topological insulators Bi_2Se_3 as saturable absorber

Yongjie Cheng[a], Jian Peng[b], Bin Xu[a], Huiying Xu[a], Zhiping Cai[a,*], Jian Weng[b]

[a] Department of Electronic Engineering, Xiamen University, Xiamen 361005, China
[b] Department of Biomaterials, Xiamen University, Xiamen 361005, China

ARTICLE INFO

Keywords:
Diode-pumped
Q-switched
Visible lasers
Nonlinear optical materials

ABSTRACT

Q-switched laser operation of a laser diode pumped $Pr:LiYF_4$ laser is reported at 604 nm using a topological insulator (TI) Bi_2Se_3 nanosheet material as saturable absorbers (SAs), for the first time to our knowledge. Stable Q-switched laser operation is obtained with shortest pulse width of about 802 ns, a maximum pulse repetition rate of 130 kHz, pulse energy of about 0.2 μJ and a maximum average output power of 26 mW. This work further extends the working wavelength of Bi_2Se_3 as saturable absorbers to visible domain.

1. Introduction

In the past two decades, much attention has been paid to visible lasers based on laser diode pumped solid state lasers (DPSSLs) technology, because DPSSLs provide efficient, robust, stable and compact laser system with excellent output laser properties. Visible lasers have great potential applications in data storage, color display, micro-sized projectors, holographic and biomedical techniques, etc. Trivalent praseodymium ion (Pr^{3+}) can generate visible laser emissions via a direct down conversion mechanism owing to its suitable emission transitions, from upper state levels of $^3P_{0,1,2}$ and $^1I_6$ to lower state levels of $^3H_{4,5,6}$ and $^3F_{2,3,4}$. Hence, Pr^{3+}-based visible lasers, in the forms of bulk [1–9], microchip [10], fiber [11], waveguide [12,13] has attracted particular attention in recent ten years.

On the other hand, with the aid of conventional saturable absorbers, e.g. Cr^{4+}:YAG crystal or semiconductor saturable absorber mirrors (SESAMs), passive Q-switching [14–16] or mode locking [17] techniques have been utilized recently to realize Pr^{3+} visible short or ultrashort pulse laser within ns down to ps time duration, which are indeed recently more and more attractive because these visible pulsed lasers can provide much higher energy for various applications that are not available for continuous-wave lasers. Despite these two above mentioned saturable absorbers are the most widely used ones, however, they have the same drawbacks: their operating wavelengths are limited to particular spectral bands. Moreover, they both require specific and expensive fabrication techniques. Moreover, except a few examples [14–17], most of these saturable absorbers have been developed only for near-infrared (NIR) wavelength domains.

During the last decade, other types of saturable absorber materials such as carbon nanotubes (CNTs) [18,19] and graphene [20–22] have been found to be very promising as saturable absorbers in fiber and DPSSLs. Therefore, efforts have been made to explore all these high-performance nanosheet materials because of their excellent properties, such as ultra-broadband saturable absorptions, low cost and easy fabrication. This is the case of these new types of nanosheet materials, Bi_2Se_3 [23–27], Bi_2Te_3 [28] and Sb_2Te_3 [29], grouped as topological insulators, as well as transition metal dichalcogenides like MoS_2 [30–32] and WS_2 [33,34]. All of them have already successfully utilized as saturable absorbers in various types of lasers.

Recently, pulsed lasers have been observed by using MoS_2 at 522 nm [35], 605 nm and 639 nm [36]. Soon later, Bi_2Se_3-based visible Q-switched laser operation has been achieved by using Pr^{3+}-ZBLAN fiber with maximum pulse energy of 22.3 nJ at 635 nm [37]. Based on this result, we expect that the Bi_2Se_3 nanosheet material can be used as Q switcher in shorter wavelengths like MoS_2. Apparently, exploiting such nanosheet saturable absorbers for passive Q-switching and even mode-locking in the visible domain is still very challenging. In this work, we show that it is possible to achieve passive Q-switching of a diode-pumped $Pr:LiYF_4$ laser operating at 604 nm by using a TI Bi_2Se_3 as saturable absorber.

2. Preparation and characterization of TI Bi_2Se_3 SA

The preparation process of few-layer TIs Bi_2Se_3 SAs is the same as we reported previously [27]. Fig. 1 shows the characterization of the as-prepared TI Bi_2Se_3. The as-prepared TI Bi_2Se_3 nanosheets are grey suspension (Fig. 1(a) inset). Atomic force microscopy (AFM) image was registered for characterizing the size and thickness of the as-prepared

* Corresponding author.
E-mail address: zpcai@xmu.edu.cn (Z. Cai).

http://dx.doi.org/10.1016/j.optlastec.2016.09.026
Received 24 March 2016; Received in revised form 5 September 2016; Accepted 14 September 2016
Available online 29 September 2016

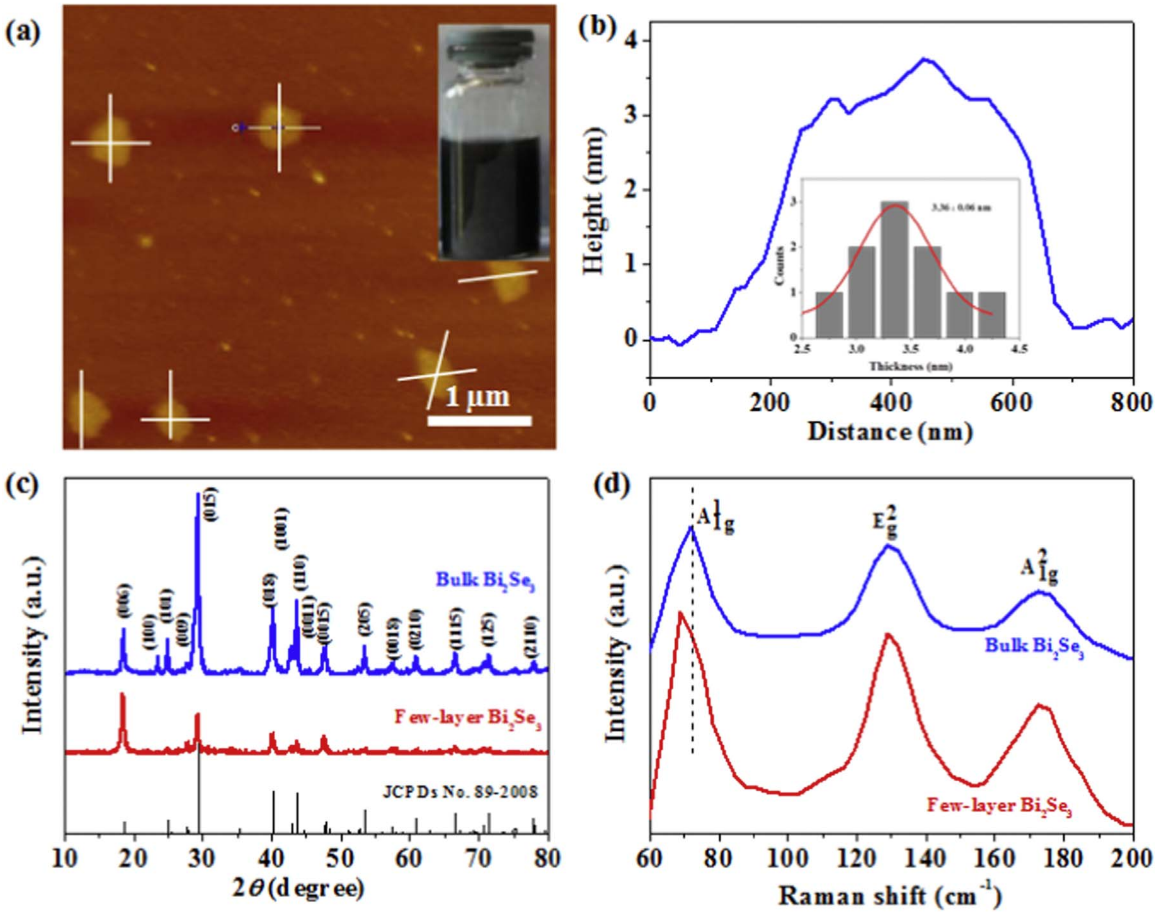

Fig. 1. (a) AFM image and photograph (inset) of as-prepared few-layer Bi_2Se_3, (b) Height profile of an as-prepared few-layer Bi_2Se_3 sample: particle size distribution was obtained by statistical analysis over 10 height profiles and the average thickness was fitted to be 3.36 nm, (c) XRD and (d) Raman spectra of the bulk Bi_2Se_3 and few-layer Bi_2Se_3 samples.

few-layer Bi_2Se_3. The size of TIs Bi_2Se_3 nanosheets are around 300–500 nm (Fig. 1(a)) and the height profile diagram (see Fig. 1(b)) shows the TI Bi_2Se_3 nanosheets are around 2–4 nm, which indicates the TI Bi_2Se_3 nanosheets are about 3 layers since the thickness of single layer is 0.96 nm [38]. The bulk Bi_2Se_3 and the as-prepared few-layer Bi_2Se_3 are both characterized by X-ray diffraction (XRD) in Fig. 1(c), in which all the labeled peaks of the bulk Bi_2Se_3 can be easily indexed to rhombohedral Bi_2Se_3 (JCPDs no. 89–2008). The bulk Bi_2Se_3 had been successfully exfoliated because the XRD pattern of the few-layer Bi_2Se_3 shows a high [006] orientation and some characteristic peaks disappeared. The Raman spectroscopy is shown in Fig. 1(d). The characteristic peaks of the bulk Bi_2Se_3 are calibrated at 72, 128 and 172 cm^{-1}. Compared with the bulk Bi_2Se_3, few-layer Bi_2Se_3 sample shows a little bit red shift of peak..

A BK7 glass was used as substrate to support the Bi_2Se_3 thin film, which was uncoated but nicely polished with surface finish quality of 60/40 (scratch/dig) and flatness of λ/4. Transmission of the glass substrate was measured to be about 92% using a Perkin Elmer Lambda 750 Spectrophotometer. The Bi_2Se_3 saturable absorber was simply achieved as follows. The Bi_2Se_3 dispersion was first dropped onto an uncoated BK7 glass substrate. Then, by a commonly used spin-coating method, the Bi_2Se_3 dispersion was uniformly distributed on the glass substrate. Finally, the sample was dried for 3 h in an oven with a temperature of 80 °C. At 604 nm, the transmission of the Bi_2Se_3 thin film onto the glass substrate was also measured to be about 81.93% (see in Fig. 2). Thus, the final transmission of the Bi_2Se_3 thin film itself could be deduced to be around 89.1%, which means that the linear loss induced by the Bi_2Se_3 thin film is about 10.9%. Saturation absorption intensity and modulation depth of the Bi_2Se_3 thin film were also measured to be about 53 MW/cm^2 and 3.8%, respectively, at 800 nm by using the same measuring setup as Ref. [23]. Thus, for laser emission at orange, saturation absorption intensity should be larger than this measured value..

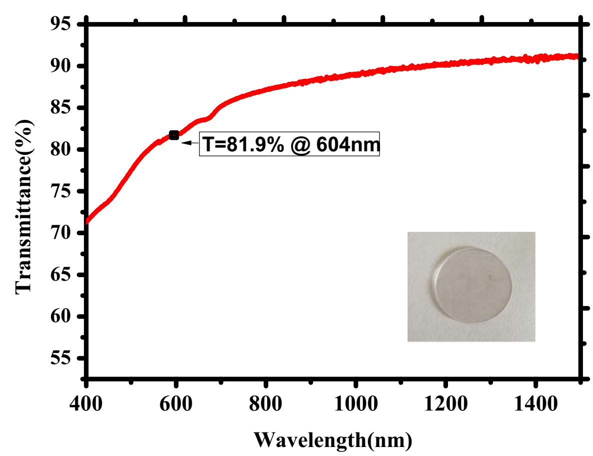

Fig. 2. The transmission of the as-prepared Bi_2Se_3 saturable absorber.

3. Experimental setup

Fig. 3 shows the schematic of the laser experimental setup. An InGaN laser diode with central wavelength of about 444 nm and maximum output power of about 2 W is used as pump source. The laser diode was integrated with an aspheric lens (focal length *f*=3 mm) for collimating the pump beam and then with a pair of cylindrical

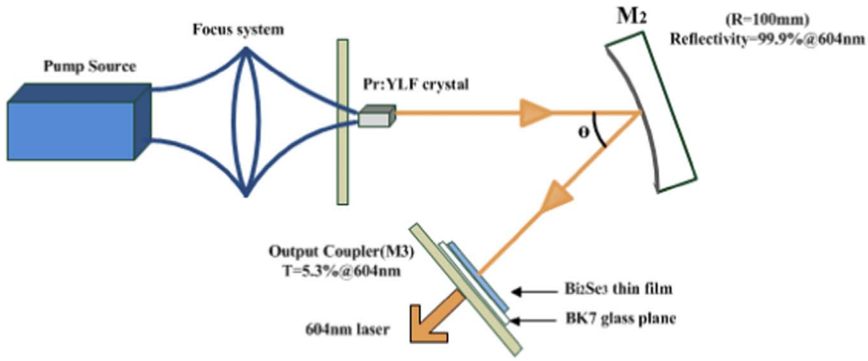

Fig. 3. Schematic experimental setup of the Bi_2Se_3-based Q-switched Pr:YLF laser at 604 nm.

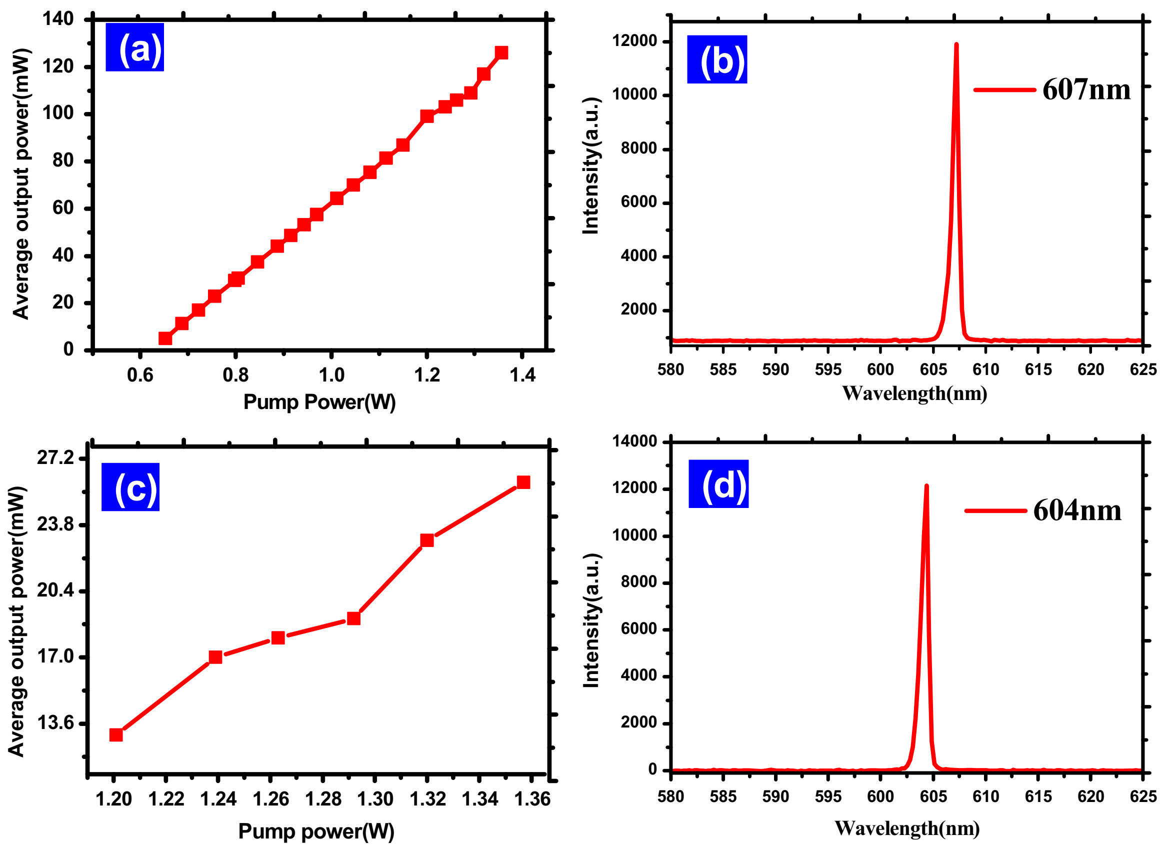

Fig. 4. Output powers and laser spectra in (a and b) continuous-wave and (c and d) Q-switching modes.

lenses (f=40 and −8 mm) for correcting the astigmatism of the pump beam. After a 50-mm (focal length) focusing lens, the pump beam was injected into the gain material, namely a 5-mm-long and 0.5 at% doped (in the crystal) Pr:YLF crystal. The laser crystal was wrapped with indium foil and mounted inside a copper block. The copper block was connected to a chiller (Huber Corp.) with temperature set at 16 °C..

The laser resonator was arranged to be a typical V-shaped three-mirror configuration. The flat input mirror M1 has a high transmission of 93.6% at the pump wavelength and a high reflection of about 99.9% at the considered orange laser wavelengths. The M2 mirror with a radius of curvature of 100 mm has also a high reflection of 99.9% at orange and a high transmission at the pump wavelength. Transmission of the flat output mirror is about 5.3% at orange. The physical cavity length was finally optimized to about 194 mm for the Q-switched operation, i.e. 109 mm for cavity arm M1–M2, as well as 85 mm for cavity arm M2–M3. In order to reduce the astigmatism produced by the curved mirror M2, the folded angle θ was set to be about 23°, the smallest angle allowed by our laser cavity. For Q-switched laser experiment, the as-prepared Bi_2Se_3 saturable absorber was inserted into the laser cavity very close to the output mirror to modulate the intracavity loss. Thus, according to a standard ABCD law, the cavity mode sizes at the gain crystal and at the Bi_2Se_3 saturable absorber were estimated to be about 90 and 72 μm, respectively.

4. Experimental results and discussions

Fig. 4(a) and (b) show continuous-wave laser operation at 607 nm (σ polarization) with a pump threshold of about 593 mW and a maximum output power of about 146 mW in free-running regime. Q-switched laser operation was fulfilled by inserting the as-prepared Bi_2Se_3 saturable absorber into the laser cavity when the laser cavity operated at continuous-wave laser threshold. Because of the additional linear loss introduced by the saturable absorber, the laser cavity can not lase any more. We therefore increased the pump power to about 873 mW and unstable Q-switching was then observed. However, stable Q-switched pulse trains was not achieved until the pump power was

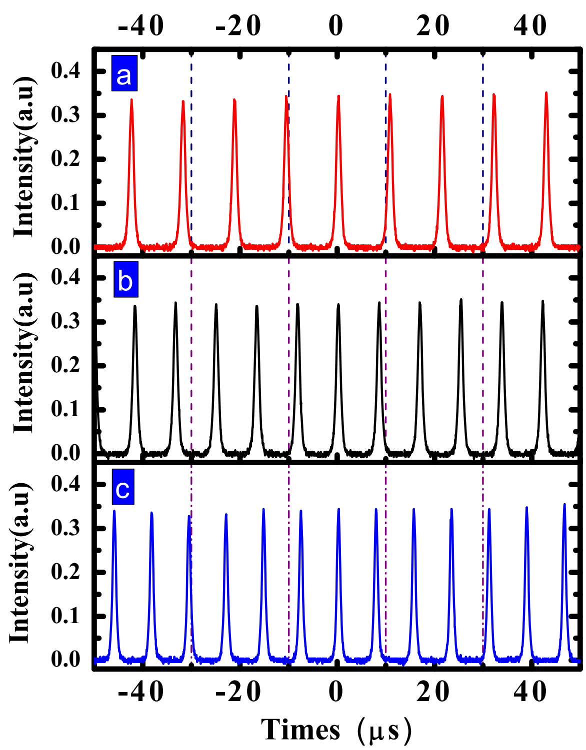

Fig. 5. Typical oscilloscope traces of the pulse trains under different pump powers: (a) 1.2 W, (b) 1.26 W and (c) 1.357 W.

augmented to about 1.2 W. The output pulsed laser wavelength was measured to be π-polarized at 604 nm, i.e. orthogonally polarized to the σ-polarized 607 nm laser, from the unstable Q switching..

We explain the 604 nm lasing instead of the 607 nm lasing in Q-switched laser operation as follows. The 604 nm line in fact has higher emission cross section than that of 607 nm line [1]. Due to the stronger reabsorption loss for 604 nm line than for 607 nm line, laser emission in general occurs at the 607 nm line. However, if the depletion of the ground state population of the Pr^{3+} ions happens by intense pumping or by operating the laser in pulse mode, thus no reabsorption loss (or much reduced) for the 604 nm line, the 604 nm lasing could occur. In fact, this phenomenon was once reported by Metz et al. [39]. These authors first obtained a 607 nm laser, but at pump power levels exceeding 3 W additional emission at 604 nm was also observed. Now, the latter case, i.e. pulse laser operation, led to the present laser operating at 604 nm.

Stable output powers of the Q-switched laser operation and laser spectrum are shown in Fig. 4(c) and (d), from which one can see that from threshold pump power of 1.2 W to pump power of 1.357 W the output powers of the Q-switching laser varied from 13 mW to maximum 26 mW. Above this pump level, Q-switching became unstable, likely because of the non-optimized transfer quality of the Bi_2Se_3 solution onto the glass substrate and of thermal load effects resulting from the poor thermal conductivity of this glass substrate.

Three typical pulse trains are shown in Fig. 5 at pump powers of 1.2 W, 1.26 W and 1.357 W, which presented that the repetition rates varied from minimum 94.2 kHz to maximum 130 kHz correspondingly. Moreover, full pulse evolutions including pulse widths and repetition rates with the pump power are also provided in Fig. 6. From the stable Q-switching threshold to the maximum output power, the pulse width decreased from about 1050–802 ns (see Fig. 7 for the achieved shortest pulse time duration), which means, for an average output power of 26 mW, a single pulse energy up to about 0.2 μJ....

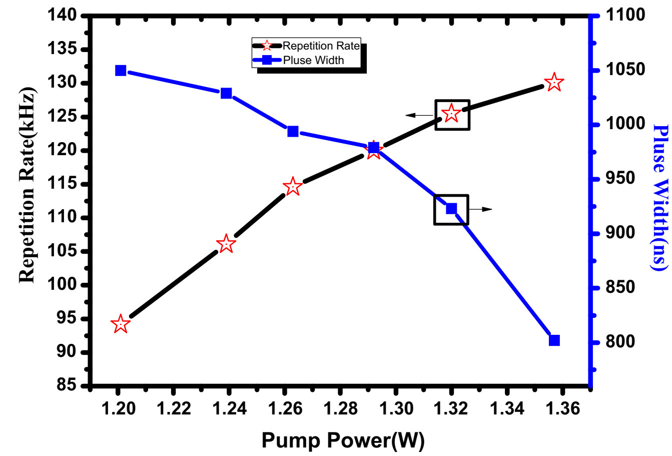

Fig. 6. Variations of pulse repetition rates and pulse widths with pump powers.

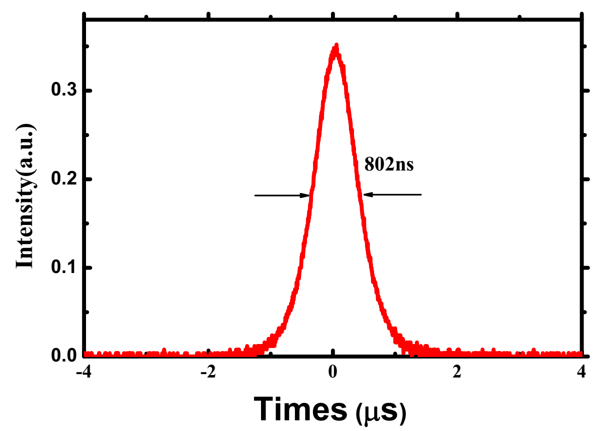

Fig. 7. The achieved narrowest pulse width at pump power of 1.357 W.

5. Conclusion

In conclusion, we demonstrated passively Q-switched laser operation of a diode-pumped $Pr:LiYF_4$ laser at π-polarized 604 nm line using Bi_2Se_3 as saturable absorbers. Stable Q-switched laser operation with a maximum average output power of about 26 mW, laser pulses of about 802 ns time duration at a maximum pulse repetition rate of 130 kHz and single pulse energy of 0.2 μJ have been achieved. This work indicated that TI Bi_2Se_3 can be applicable in producing Q-switched lasers at wavelengths down to orange spectral domain. Further better laser performance of the Q-switching can be expected by optimizing the transfer quality and thermal effect of the TI Bi_2Se_3 thin film. Bi_2Se_3-based mode locking visible lasers is also under investigation in our lab.

Acknowledgement

The authors also wish to acknowledge the financial support partly from the National Natural Science Foundation of China (61275050, 61575164), the Specialized Research Fund for the Doctoral Program of Higher Education (20120121110034, 20130121120043), the Fundamental Research Funds for the Central Universities (2013121022) and Natural Science Foundation of Fujian Province of China (2014J01251).

References

[1] A. Richter, E. Heumann, E. Osiac, G. Huber, W. Seelert, A. Diening, Diode pumping of a continuous-wave Pr^{3+}-doped $LiYF_4$ laser, Opt. Lett. 29 (22) (2004) 2638.

[2] B. Xu, P. Camy, J.L. Doualan, Z.P. Cai, R. Moncorgé, Visible laser operation of Pr^{3+}-doped fluoride crystals pumped by a 469 nm blue laser, Opt. Express 19 (2) (2011)

1191–1197.
[3] B. Xu, F. Starecki, D. Paboeuf, P. Camy, J.L. Doualan, Z.P. Cai, A. Braud, R. Moncorgé, pH Goldner, F. Bretenaker, Red and orange laser operation of Pr:KYF_4 pumped by a Nd: YAG/LBO laser at 469.1 nm and a InGaN laser diode at 444 nm, Opt. Express 21 (5) (2013) 5567–5574.
[4] B. Xu, Z. Liu, H.Y. Xu, Z.P. Cai, C.H. Zeng, S.L. Huang, Y. Yan, F.J. Wang, S.Y. Luo, P. Camy, J.L. Doualan, A. Braud, R. Moncorgé, High-efficiency InGaN-LD-pumped bulk Pr:YLF orange laser at 607 nm, Opt. Commun. 305 (2013) 96–99.
[5] Z. Liu, Z.P. Cai, S.L. Huang, C.H. Zeng, Z. Meng, Y.K. Bu, Z.Q. Luo, B. Xu, H.Y. Xu, C.C. Ye, F. Stareki, P. Camy, R. Moncorgé, Diode-pumped Pr^{3+}:$LiYF_4$ continuous-wave deep red laser at 698 nm, J. Opt. Soc. Am. B 30 (2) (2013) 302.
[6] Y.J. Cheng, B. Xu, B. Qu, S.Y. Luo, H. Yang, H.Y. Xu, Z.P. Cai, Comparative study on diode-pumped continuous wave laser at 607 nm using differently doped Pr^{3+}:$LiYF_4$ crystals and wavelength tuning to 604 nm, Appl. Opt. 53 (33) (2014) 7898.
[7] B. Qu, B. Xu, S.Y. Luo, Y.J. Cheng, H.Y. Xu, Z.P. Cai, P. Camy, J.L. Doualan, R. Moncorgé, InGaN-LD-pumped continuous-wave deep red laser at 670 nm in Pr^{3+}:$LiYF_4$ crystal, IEEE Photonics Technol. Lett. 27 (4) (2015) 333–335.
[8] P. Camy, J.L. Doualan, R. Moncorgé, J. Bengoechea, U. Weichmann, Diode-pumped Pr^{3+}:KY_3F_{10} red laser, Opt. Lett. 32 (11) (2007) 1462.
[9] T. Gün, P. Metz, G. Huber, Power scaling of laser diode pumped Pr^{3+}:$LiYF_4$ cw lasers: efficient laser operation at 522.6 nm, 545.9 nm, 607.2 nm, and 639.5 nm, Opt. Lett. 36 (6) (2011) 1002.
[10] M. Fibrich, H. Jelinkova, J. Sulc, K. Nejezchleb, V. Skoda, Pr:$YAlO_3$ microchip laser, Opt. Lett. 35 (15) (2010) 2556.
[11] H. Okamoto, K. Kasuga, I. Hara, Y. Kubota, Visible-NIR tunable Pr^{3+}-doped fiber laser pumped by a GaN laser diode, Opt. Express 17 (22) (2009) 20227.
[12] F. Starecki, W. Bolaños, A. Braud, J.L. Doualan, G. Brasse, A. Benayad, V. Nazabal, B. Xu, R. Moncorgé, P. Camy, Red and orange Pr^{3+}:$LiYF_4$ planar waveguide laser, Opt. Lett. 38 (4) (2013) 455.
[13] S. Müller, T. Calmano, P. Metz, N.O. Hansen, C. Kränkel, G. Huber, Femtosecond-laser-written diode-pumped Pr:$LiYF_4$ waveguide laser, Opt. Lett. 37 (24) (2012) 5223.
[14] R. Abe, J. Kojou, F. Kannari, Saturable absorption of Cr:YAG crystal in visible region for passively Q-switched Pr:YLF Laser, Adv. Photonics Congr. 21 (2012) (JTu5A).
[15] R. Abe, J. Kojou, K. Masuda, F. Kannari, Cr^{4+}-Doped $Y_3Al_5O_{12}$ as a saturable absorber for a Q-Switched and mode-locked 639-nm Pr^{3+}-Doped $LiYF_4$ Laser, Appl. Phys. Express 6 (1992) 032703.
[16] V.G. Savitski, I.M. Ranieri, A.B. Krysa, S. Calvez1, Passively Q-switched Pr:YLF laser, CLEO(OSA), CMB7, 2011.
[17] M. Gaponenko, P.W. Metz, A. Härkönen, A. Heuer, T. Leinonen, M. Guina, T. Südmeyer, G. Huber, C. Kränkel, SESAM mode-locked red praseodymium laser, Opt. Lett. 39 (24) (2014) 6939–6941.
[18] S.Y. Set, H. Yaguchi, Y. Tanaka, M. Jablonski, Y. Saka kibara, A. Rozhin, M. Tokumoto, H. Kataura, Y. Achiba, K. Kikuchi, Mode-locked fiber lasers based on a saturable absorber incorporating carbon nanotubes, OSA/OFC, PD44, 2003.
[19] A. Schmidt, S. Rivier, G. Steinmeyer, J.H. Yim, W.B. Cho, S. Lee, F. Rotermund, M.C. Pujol, X. Mateos, M. Aguiló, F. Díaz, V. Petrov, U. Griebner, Passive mode locking of Yb:KLuW using a single-walled carbon nanotube saturable absorber, Opt. Lett. 33 (7) (2008) 729–731.
[20] Z.Q. Luo, M. Zhou, J. Weng, G. Huang, H.Y. Xu, C.C. Ye, Z.P. Cai, Graphene-based passively Q-switched dual-wavelength erbium-doped fiber laser, Opt. Lett. 35 (21) (2010) 3709–3711.
[21] W.D. Tan, C.Y. Su, R.J. Knize, G.Q. Xie, L.J. Li, D.Y. Tang, Mode locking of ceramic Nd: yttrium aluminum garnet with graphene as a saturable absorber, Appl. Phys. Lett. 96 (2010) 031106.
[22] J.L. Xu, X.L. Li, J.L. He, X.P. Hao, Y. Yang, Y.Z. Wu, S.D. Liu, B.T. Zhang, Efficient graphene Q switching and mode locking of 1.34 µm neodymium lasers, Opt. Lett. 37 (2012) 2652–2654.
[23] Z.Q. Luo, Y.Z. Huang, J. Weng, H.H. Cheng, Z.Q. Lin, B. Xu, Z.P. Cai, H.Y. Xu, 1.06 µm Q-switched ytterbium-doped fiber laser using few-layer topological insulator Bi_2Se_3 as a saturable absorber, Opt. Express 21 (2013) 29516–29522.
[24] H.H. Yu, H. Zhang, Y.C. Wang, C.J. Zhao, B.L. Wang, S.C. Wen, H.J. Zhang, J.Y. Wang, Topological insulator as an optical modulator for pulsed solid-state lasers, Laser Photonics Rev. 7 (2013) L77–L83.
[25] B.L. Wang, H.H. Yu, H. Zhang, C.J. Zhao, S.C. Wen, H.J. Zhang, J.Y. Wang, Topological insulator simultaneously Q-switched dual-wavelength Nd: Lu_2O_3 Laser, IEEE Photonics J. 6 (2014), 2014, p. 1501007.
[26] C.J. Zhao, Y.H. Zou, Y. Chen, Z.T. Wang, S.B. Lu, H. Zhang, S.C. Wen, D.Y. Tang, Wavelength-tunable picosecond soliton fiber laser with topological insulator: Bi_2Se_3 as a mode locker, Opt. Express 20 (25) (2012) 27888.
[27] B. Xu, Y. Wang, J. Peng, Zh Luo, H. Xu, Zh Cai, J. Weng, Topological insulator Bi_2Se_3 based Q-switched Nd:$LiYF_4$ nanosecond laser at 1313 nm, Opt. Express 23 (6) (2015) 7674.
[28] P.H. Tang, X.Q. Zhang, C.J. Zhao, Y. Wang, H. Zhang, D.Y. Shen, S.C. Wen, D.Y. Tang, D.Y. Fan, Topological insulator: Bi_2Te_3 saturable absorber for the passive Q-switching operation of an in-band pumped 1645-nm Er:YAG ceramic laser, IEEE Photonics J. 5 (2013) 1500707.
[29] J. Sotor, G. Sobon, K. Grodecki, K.M. Abramski, Mode-locked erbium-doped fiber laser based on evanescent field interaction with Sb_2Te_3 topological insulator, Appl. Phys. Lett. 104 (2014) 251112.
[30] S. Wang, H. Yu, H. Zhang, A. Wang, M. Zhao, Y. Chen, L. Mei, J. Wang, Broadband few-layer MoS_2 saturable absorbers, Adv. Mater. 26 (2014) 3538.
[31] Z. Luo, Y. Huang, M. Zhong, Y. Li, J. Wu, B. Xu, H. Xu, Zh Cai, J. Peng, J. Weng, 1-, 1.5-, and 2-µm fiber lasers Q-switched by a broadband few-layer MoS_2 saturable absorber, J. Lightwave Technol. 32 (24) (2014) 4077.
[32] B. Xu, Y. Cheng, Y. Wang, Y. Huang, J. Peng, Z. Luo, H. Xu, Z. Cai, J. Weng, R. Moncorgé, Passively Q-switched Nd:$YAlO_3$ nanosecond laser using MoS_2 as saturable absorber, Opt. Express 22 (23) (2014) 28934.
[33] D. Mao, Y. Wang, C. Ma, L. Han, B. Jiang, X. Gan, S. Hua, W. Zhang, T. Mei, J. Zhao, WS_2 mode-locked ultrafast fiber laser, Sci. Rep. 5 (2015) 7965.
[34 P. Yan, A. Liu, Y. Chen, H. Chen, S. Ruan, C. Guo, S. Chen, I. Ling Li, H. Yang, J. Hu, G. Cao, Microfiber-based WS_2-film saturable absorber for ultra-fast photonics, Opt. Mater. Express 5 (3) (2015) 479.
[35] Y. Zhang, S. Wang, D. Wang, H. Yu, H. Zhang, Y. Chen, L. Mei, Alberto Di Lieto, Mauro Tonelli, J. Wang, Atomic-Layer molybdenum sulfide passively modulated green laser pulses, IEEE Photonics Technol. Lett. 28 (2) (2016) 197.
[36] Y. Zhang, S. Wang, H. Yu, H. Zhang, Y. Chen, L. Mei, Alberto Di Lieto, Mauro Tonelli, J. Wang, Atomic-layer molybdenum sulfide optical modulator for visible coherent light, Sci. Rep. 5 (11342) (2015) 1.
[37] D. Wu, Z. Cai, Y. Zhong, J. Peng, J. Weng, Z. Luo, N. Chen, H. Xu, 635-nm Visible Pr^{3+}-doped ZBLAN fiber lasers Q-switched by topological insulators SAs, IEEE Photonics Technol. Lett. 27 (22) (2015) 2379.
[38] Y. Sun, H. Cheng, S. Gao, Q. Liu, Z. Sun, C. Xiao, C. Wu, S. Wei, Y. Xie, Atomically thick bismuth selenide freestanding single layers achieving enhanced thermo-electric energy harvesting, J. Am. Chem. Soc. 134 (2012) 20294–20297.
[39] Philip Werner Metz, Fabian Reichert, Francesca Moglia, Sebastian Müller, Daniel-Timo Marzahl, Christian Kränkel, G.ünter Huber, High-power red, orange, and green Pr^{3+}:$LiYF_4$ lasers, Opt. Lett. 39 (11) (2014) 3193.